NIPPON STEEL TECHNICAL REPORT No. 100 JULY 2011

Technical Report

UDC 543 . 5 : 621 . 375 . 826

Rapid Inspection of Defects of Steel by Laser Induced Breakdown Spectroscopy

Hiroyuki KONDO* Michihiro AIMOTO
Hideaki YAMAMURA Takehiko TOH

Abstract

A rapid and simple technique has been developed for inspection of defects of steel using laser induced breakdown spectroscopy (LIBS). Irradiation from a Q-switched Nd:YAG laser was focused onto the sample surface by a plano-convex lens with a spot diameter of about 1mm to ablate a portion of sample and generate a micro plasma. Emission from the plasma was transmitted by a fiber optics to a Paschen-Runge mounting polychrometer. Each sample was analyzed at two points, normal and defect parts and these two analytical results were compared with each other. Typical elements could be detected at defect part with significantly high intensities for different types of inclusion; Al for alumina, Al, Ca, Mg, Si, Na for mold flux and Al, Ca, Mg for slag. Therefore, type of non-metallic inclusion causing the defect could be attributed by LIBS. An evaluation time was within 30 minutes including sample preparation. The developed method was also applied to elemental mapping of central segregation of slabs.

1. Introduction

Defects in steel materials adversely affect the quality and yield of products constructed from them. Therefore, in steelmaking processes, developing a technology that permits speedy determination of the causes of defects is as important as developing equipment technology related to defect prevention, such as continuous casting that applies an electromagnetic stirrer and a level magnetic field to control surface defects and center segregations.[1)]

Surface defects in rolled steel are not limited to mechanical defects, including roll marks. There are various other surface defects: mold flux-induced defects ascribable to the penetration into steel of the mold flux added as mold lubricant in the continuous casting process; alumina-induced defects due to nonmetallic inclusions in steel caused by excessive oxidation and outflow of converter slag into the ladle in the refining process or insufficient floating of alumina in the vacuum degassing equipment (RH); and slag-induced defects resulting from nonmetallic inclusions ascribable to the entanglement of slag in the tundish. In addition, there are defects ascribable to insufficient removal of scale from the steel surface after operation of the reheating furnace. It is important to speedily investigate the cause of each of these defects and identify which manufacturing process needs to be corrected.

Once the cause of a specific defect is identified, it is possible to implement suitable remedial measures without delay. Examples of them are stabilization of the mold bath level and optimization of the electromagnetic stirrer of the mold bath for mold flux-induced defects; prevention of excessive decarburization of steel in the converter, improvement of the quality of slag, and/or taking a suitable circulation time after RH deoxidation for alumina-induced defects; ensuring of sufficient time for slag to float in the tundish for slag-induced defects; and optimization of the reheating furnace tempera-

* Senior Researcher, Materials Characterization Research Lab., Advanced Technology Research Laboratories
20-1, Shintomi, Futtsu, Chiba

ture, enhancement of the descaling capacity, etc. for scale-induced defects.

Concerning center segregations that can occur during solidification of a slab, there are concerns that they will be carried over to the product in the form of internal defects in the steel sheet. Therefore, if center segregations could be detected as a slab is being cast, imprudent use of the material can be avoided, resulting in making the most effective use of it.

So far, various methods have been used to investigate the causes of defects in steel. For surface defects, cross sections of defective parts are observed using optical microscopy and EPMA (electron probe micro-analysis) or EDX (energy-dispersive X-ray spectroscopy). Center segregations are observed by means of macroscopic examination by etching, etc.[2] These and other conventional methods require complicated and time-consuming preparation of the sample (e.g., cutting and polishing). Besides, they are not very reliable because the substance that is the cause of the defect might come off the sample during sample preparation or it might be overlooked during observation of a specific cross section of the sample. Therefore, the results of investigations using them would hardly be able to be fed back to manufacturing operations speedily and properly.

As new techniques to swiftly investigate the causes of defects, there is laser ablation ICP (inductively coupled plasma) emission spectrometry[3] and elemental mapping by spark emission spectrometry.[4] It has been reported that both methods are very effective for examining surface defects in steel sheet. However, laser ablation ICP emission spectrometry requires a somewhat complicated system, which is rather difficult to operate and maintain. On the other hand, elemental mapping by spark emission spectrometry, which utilizes a spark discharge, requires delicate control at the point of discharge according to the sample shape and structure.

Laser-induced breakdown spectroscopy (LIBS) is an analytical technique to obtain information about elements in the target substance by observing the emission lines of wavelengths specific to each element that are emitted in the process of relaxation of atoms that are collision-excited by electrons, etc. in hot plasma generated by a laser pulse with a high peak power.[5, 6] Since LIBS does not require any special chemical pretreatment, sample preparation is easy and limitations on the sample shape are relatively modest. The main devices required for LIBS are a laser and a spectrometer. Therefore, it is possible to configure a compact LIBS system. Besides, LIBS does not require special skill.

Examples of elemental mapping implemented using LIBS include: mapping of MnS in steel sheet;[7] mapping of nonmetallic inclusions on the surface of stainless steel sheet by laser line scanning;[8] mapping of inclusions in aluminum alloy;[9] etc. As examples of depth profiling, there is LIBS analysis of plating layers.[10, 11] However, none of the above studies was conducted from the standpoint of determining the causes of defects. In the present study, we discussed the possibility of applying LIBS to speedily determine the causes of defects and analyze center segregations in steel focusing our attention on the advantageous characteristics of LIBS, which does not require burdensome chemical or physical pretreatment.

2. Experimental

2.1 Experimental apparatus

The experimental apparatus is presented schematically in **Fig. 1**. A Q-switched Nd:YAG laser beam (Continuum Surelite III-10; wavelength: 532 nm, pulse width: 12 ns, pulse repetition frequency: 10 Hz), focused by a plano-convex lens having a focal length of 80 mm, was irradiated onto the surface of the sample to generate micro-plasma by evaporating and atomizing part of the sample. The spot diameter at the sample surface was about 1 mm, and the pulse energy was 100 mJ. Emissions from the plasma were transmitted over an optical fiber cable to a Paschen-Runge polychrometer (Shimadzu Corporation; focal length: 500 mm) for spectroscopic measurement. Detected photo intensities were integrated with a delay time of 10 μs against the laser pulse. We paid special attention to elements composing nonmetallic inclusions. The analytical lines for these elements are shown in **Table 1**.

Fig. 2 shows the Al calibration curve we prepared using JSS-certified reference materials with our LIBS system. The linearity of the calibration line was good in the range from 10 to 780 μg/g-Al. From this, we could confirm that it would be possible to quantitatively evaluate the difference in element concentration in the sample.

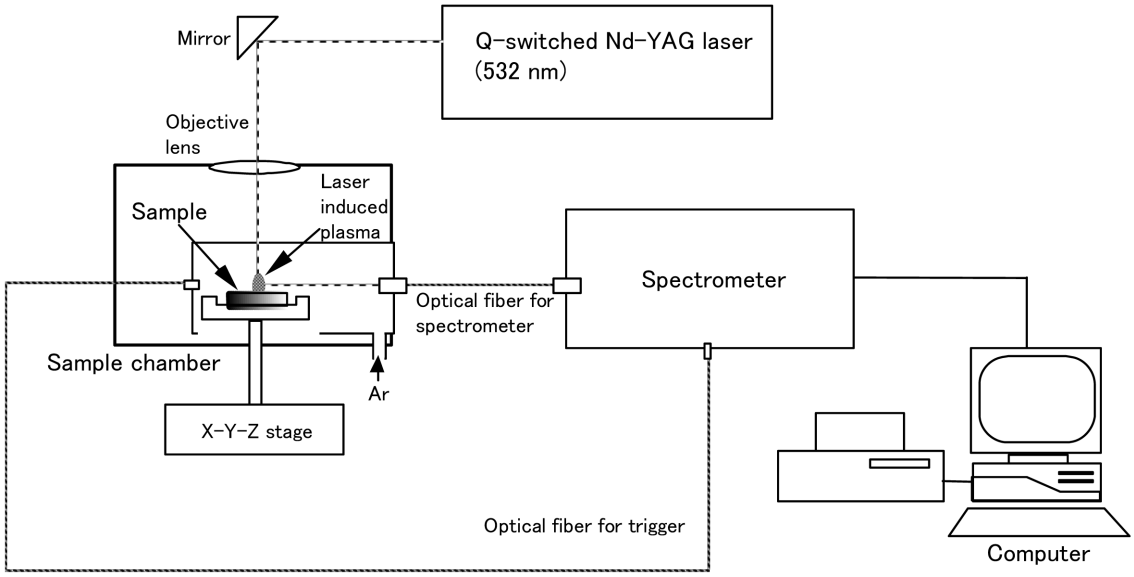

Fig. 1 Schematic diagram of LIBS system

Table 1 Analytical lines

Element	Analytical line (nm)
Si I	252.4
Mg II	279.6
Ca II	393.4
Al I	396.2
Al I	309.3
Na I	589.0
Zn I	303.6
Fe I	310.1
C I	193.1
S I	180.7

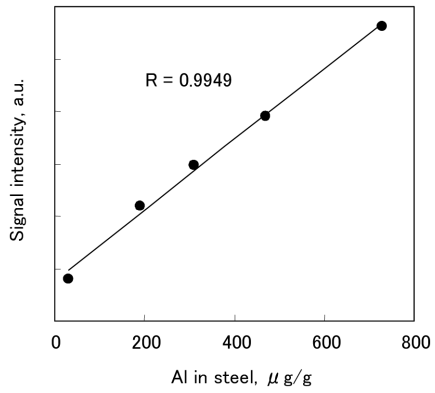

Fig. 2 Calibration curve of Al in steel by LIBS

2.2 Samples and analytical method

(1) Surface defects of steel sheets

We analyzed four galvanized sheets (Samples A, B, C, and D) whose surface defects could be observed with the unaided eye. Each of the samples was fixed on the X-Y stage inside the laser irradiation chamber, which was filled with atmospheric Ar. As shown in **Fig. 3**, both the normal and the defective parts were analyzed and the results were compared. In order to verify the analysis results obtained by LIBS, we observed cross sections of the defective parts by EPMA and compared them.

(2) Sample with center segregation

A sample containing center segregation was cut out from a slab of low-alloy steel. The segregated part of the sample was previously confirmed by the etching method. After the etched layer of sample surface was belt-polished, it was analyzed.

In the experiment, while the sample fixed to the X-Y stage was scanned, the laser beam was irradiated onto points of 18 × 8 at pitches of 1 mm (300 pulses per point) for semi-quantitative mapping of element concentrations at the sample surface. It was considered that more C, S, Mn, and P, having a small solid-liquid partition coefficient, would be concentrated in the center-segregated part than other elements. In the present experiment, therefore, we assumed C and S to be elements that are easily concentrated, and Si, Al, and Ca to be elements that are reluctantly concentrated.

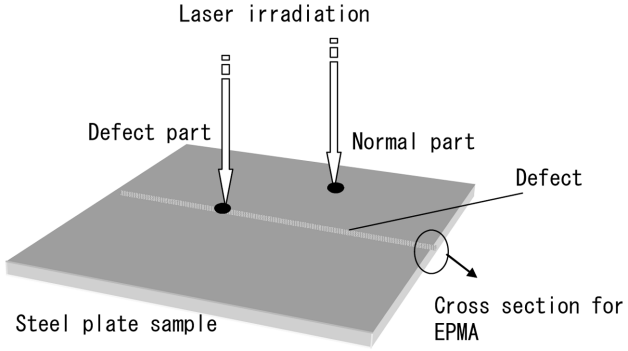

Fig. 3 Sample and laser irradiation positions

3. Experimental Results and Discussion

3.1 Surface defects of steel sheets

The emission intensities of Si, Al, and Ca obtained by analyzing the normal part (○) and defective part (×) of each of Samples A, B, and D are shown in **Figs. 4** (i), (ii), and (iii). Each of the measured values shown in Fig. 4 is an integral intensity for 300 pulses, which has been normalized by the averaged values obtained by analyzing the normal part several times. As shown in Fig. 4 (i), in Sample A, Ca was clearly detected in the defective part. Si and Al also showed rather strong emissions in the defective part of the sample.

The above results suggest that CaO exists in the defective part of Sample A. CaO is contained in both mold flux and slag. Looking at Fig. 4 (ii), on the other hand, in Sample B, there is very little difference in Ca intensity between the normal and the defective parts, whereas only Al was strongly detected in the defective part. From this, it was assumed that the defect in Sample B was ascribable to alumina. Concerning Sample D, as shown in Fig. 4 (iii), there was little difference in the intensity of Si, Al, or Ca between the normal and the defective parts. Therefore, it was assumed that the defect in Sample D was a scale defect, that is, an oxide film remaining on the sheet surface.

The emission intensities for each of Na, Mg, Al, Si, Ca, Zn, and Fe per pulse measured by irradiating a laser beam to the normal and

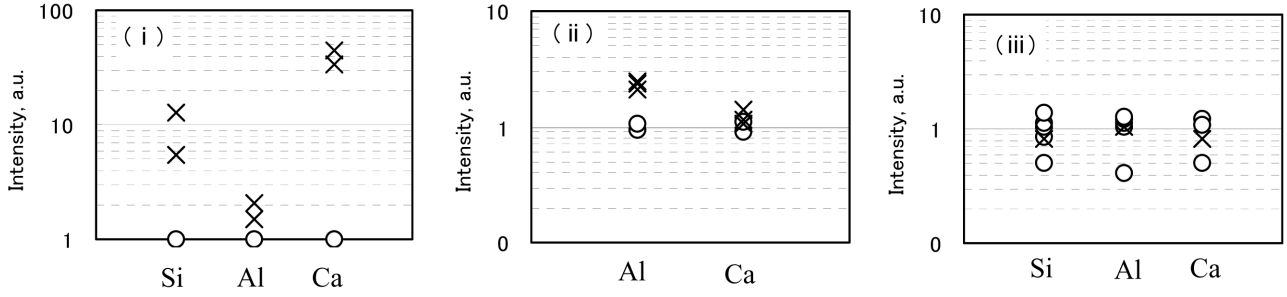

Fig. 4 Analytical results by LIBS for sample (A) (i), (B) (ii) and (D) (iii) obtained with normal (○) and defect (×) part, respectively

defective parts of Sample A are shown in **Figs. 5** (i) and (ii). In the defective part, the intensities of Na, Mg, and Ca are much higher than those in the normal part. Since these elements are characteristic of mold flux, the defect in Sample A was judged to be caused by mold flux entrapped in the steel during casting. It should be noted that in the present analysis method, it is unnecessary to remove the sheet of the plating layer, which is naturally removed during irradiation by a laser beam. From Fig. 5 (i), it can be seen that the boundary between the plating layer and the substrate is located in the neighborhood of 100 pulses. At the boundary, a concentration of Al caused by the formation of Fe-Al alloy is observed. The depth profile of each element at the individual analysis points can be obtained in about 60 seconds and hence, each sample can be analyzed in 120 seconds.

The results of depth profiling of the normal and defective parts of Sample C are shown in **Figs. 6** (i) and (ii). For the purpose of simplification, the analysis results for Zn and Fe have been omitted. A comparison between Fig. 6 (i) and (ii) revealed that Al, Mg, and Ca were conspicuously detected in the defective part, but that there was no difference in Na intensity between the normal and the defective parts. Therefore, we judged that the defect in Sample C was ascribable to slag.

The EPMA results for the defective parts of Samples A and C are shown in **Figs. 7 and 8**. Sample A shows segregations of Ca, Mg, Si, and Na, whereas Sample C shows segregations of Al, Mg, and Ca. These elements were found to be the same as the elements that were confirmed to have been concentrated in the parts analyzed by LIBS.

3.2 Center segregation of slab

Fig. 9 shows elemental maps of the sample with center segregation. A laser beam was irradiated onto the points of intersection of the grid lines. As mentioned earlier, the interval of laser irradiation was 1 mm. In the figure, the dark portions showing high signal intensities represent the segregation of an element. It can be seen that C and S segregated and that Si was slightly concentrated. Although Al and Ca were also measured, their concentrations were not confirmed. Concerning Fe, the matrix, the signal intensities obtained were almost the same at all measuring points, except that the segregated part showed slightly higher signal intensity. Thus, we were unable to observe any influence of the structure of the sample or of the elements coexisting in the sample. Although we did not test this in the present study, it is considered possible to obtain more detailed information about the condition of slab segregation by increasing the number of elements measured (Mn, P, etc.) and/or improving the 2-dimensional resolution by narrowing the diameter of the laser irradiation spot.

4. Conclusion

We developed a new technique to rapidly investigate the causes of defects in steel using LIBS. By comparing the analysis results between the normal and the defective parts of a sample, it is possible

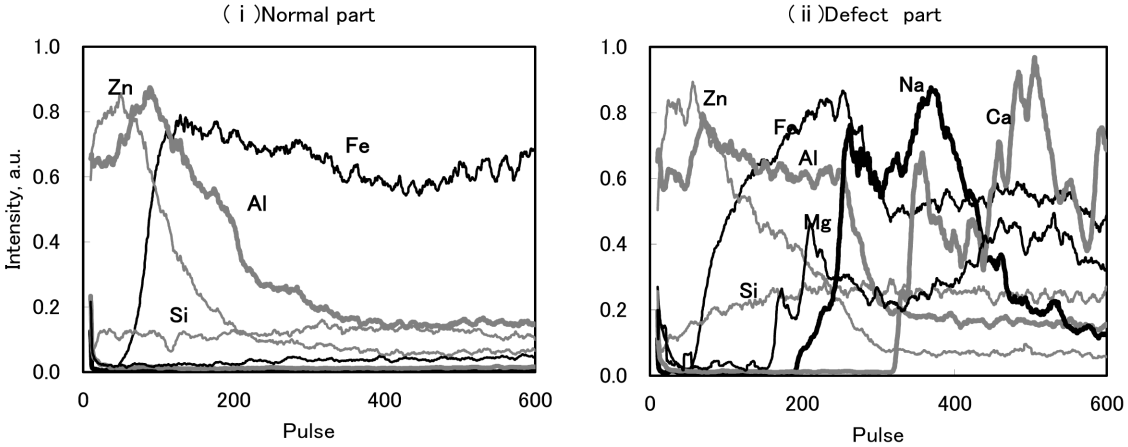

Fig. 5 Depth profiles by LIBS for sample (A) obtained at normal part (i) and defect part (ii)

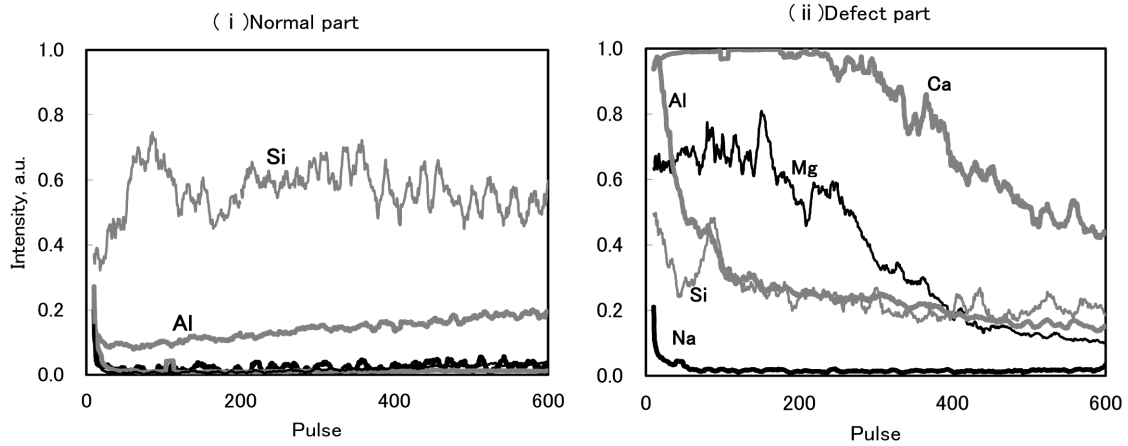

Fig. 6 Depth profiles by LIBS for sample (C) obtained at normal part (i) and defect part (ii)

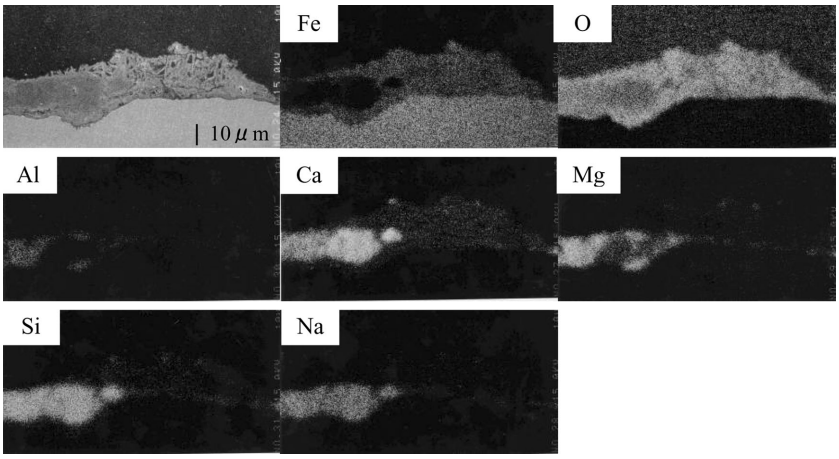

Fig. 7 EPMA results for sample (A) (× 1 000)

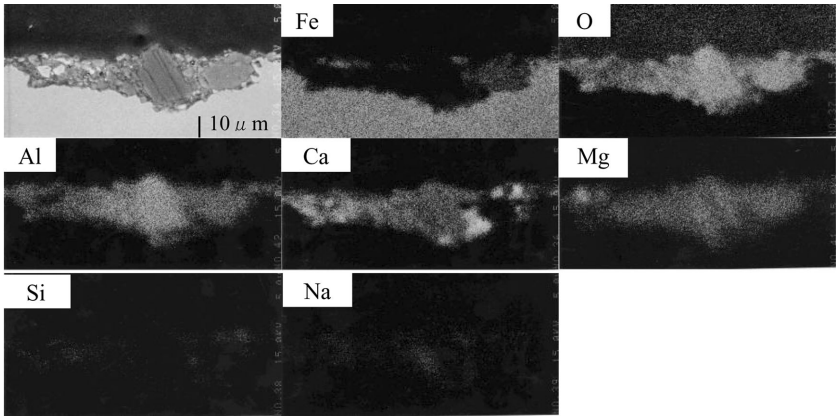

Fig. 8 EPMA results for sample (C) (× 1 000)

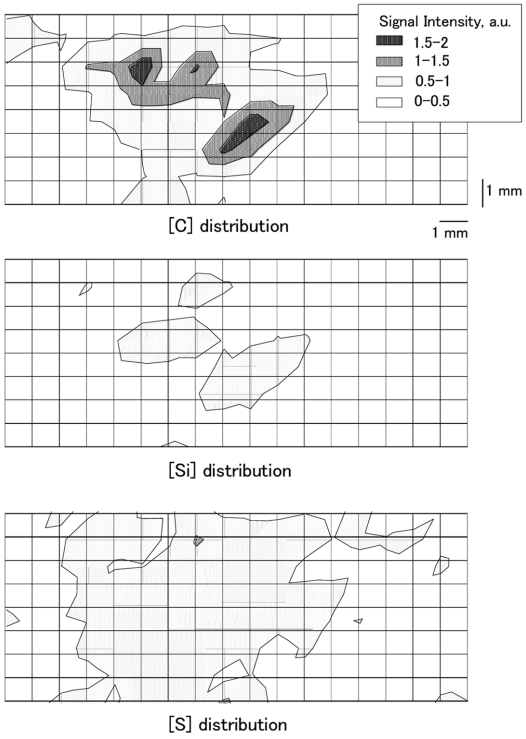

Fig. 9 Elemental mapping results of central segregation

to determine whether the defect is ascribable to certain nonmetallic inclusions (alumina, slag, or mold flux) or to residual scale. With our new technique, the cause of a defect of a given sample can be determined within 30 minutes, including the time required for sample preparation. Hence, it permits the taking of speedy and appropriate action in the manufacturing process. We expect that it will help improve the quality and productivity of steel materials.

References

1) Toh, T.: 57th Shiraishi Memorial Lecture. Iron and Steel Institute of Japan, Tokyo, 2006, p. 41
2) JIS G 0553, 1996
3) Mochizuki, T. et al.: CAMP-ISIJ. 9 (4, 6), 800 (1996)
4) Meilland, R. et al.: La Revue de Metallurgie. 4, 373 (2002)
5) Tognoli, E. et al.: Spectrochimica Acta. 57B (7), 1115 (2002)
6) Wong, D. M. et al.: Encyclopedia of Spectroscopy and Spectrometry. 1st ed. Academic Press, Maryland Heights, 2009, p. 1281
7) Noll, R. et al.: Spectrochim. Acta. 56B (6), 637 (2001)
8) Mateo, M. P. et al.: Spectrochim. Acta. 57B (3), 601 (2002)
9) Cravetchi, I. V. et al.: Spectrochim. Acta. 59B (9), 1439 (2004)
10) St-Onge, L. et al.: Spectrochim. Acta. 55B (3), 299 (2000)
11) Balzer, H. et al.: Spectrochim. Acta. 60B (7-8), 1172 (2005)

Hiroyuki KONDO
Senior Researcher,
Materials Characterization Research Lab.,
Advanced Technology Research Laboratories
20-1, Shintomi, Futtsu, Chiba

Michihiro AIMOTO
Senior Researcher,
Materials Characterization Research Lab.,
Advanced Technology Research Laboratories

Hideaki YAMAMURA
Chief Researcher,
Steelmaking Research & Development Division,
Environment and Process Technology Center

Takehiko TOH
Chief Researcher,
Steelmaking Research & Development Division,
Environment and Process Technology Center
(now the Mathematical Science & Technology
Research Lab., Advanced Technology Research
Laboratories)